Journal of Sound and Vibration (2003) **259**(1), 219–228
doi:10.1006/jsvi.2002.5133, available online at http://www.idealibrary.com on IDEAL®

FREE VIBRATION ANALYSIS OF ORTHOTROPIC RIGHT CANTILEVER TRIANGULAR PLATES

T. Sakiyama, M. Huang, H. Matsuda and C. Morita

Department of Structural Engineering, Nagasaki University, Bonkyo Machi 1-14*, Nagasaki* 852-8521*, Japan. E-mail: sakiyama@st.nagasaki-u.ac.jp*

(*Received* 3 *December* 2001, *and in final form* 20 *March* 2002)

1. INTRODUCTION

Free vibration problems of isotropic triangular plates have been studied for many years. Early studies were well compiled in reference [1]. Further studies have been done for the past two decades [2–10]. With the increasing use of orthotropic materials in engineering, the study of free vibration problems of orthotropic triangular plates has received more and more attention [7, 11–13]. Compared with the study of the vibration problems of isotropic triangular plates, the study of orthotropic triangular plates is rather limited.

In this note, an approximate method is proposed for analyzing the free vibration of orthotropic right cantilever triangular plate. By adding an extremely thin part, a cantilever triangular plate can be translated into an equivalent rectangular plate with non-uniform thickness. Therefore, the free vibration characteristics of the triangular plate can be obtained by analyzing the equivalent rectangular plate. The characteristic equation of the free vibration is obtained by using the Green function, which is the discrete-form solution [14] for the deflection of the plate with a concentrated load at each discrete point. The lowest eight frequencies and their mode shapes are shown for some orthotropic right cantilever triangular plates with various aspect ratios and variable thickness. The efficiency and accuracy of the numerical solutions by the proposed method are investigated.

2. EQUIVALENT RECTANGULAR PLATE OF A RIGHT CANTILEVER TRIANGULAR PLATE

A right cantilever triangular plate is quite different from a uniform rectangular plate, but it can be translated into an equivalent rectangular plate with non-uniform thickness (shown in Figure 1) by adding an extremely thin part to the original part.

In this note, the thickness of the original part is expressed by h, and the thickness of the extremely thin part is expressed as h_t. The fixed and free edges are denoted by the symbols C and F, respectively, and are shown by solid and dotted lines. The first symbol indicates the conditions at $x=0$, the second at $y=0$ and the third at the hypotenuse. The plate CFF is analyzed in the present study.

After the equivalent rectangular plate is obtained, all the analyses are carried out on the equivalent rectangular plate.

0022-460X/02/$35.00

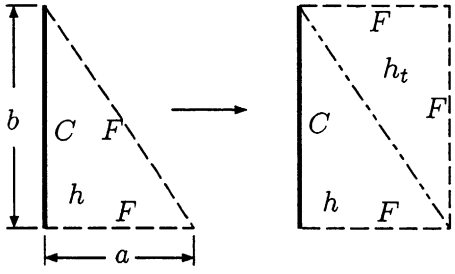

Figure 1. Cantilever right triangular plate and its equivalent rectangular plate.

3. DISCRETE GREEN FUNCTION

An xyz co-ordinate system is used in the present study with its x–y plane contained in the middle plane of an orthotropic rectangular plate and the z-axis perpendicular to the middle plane of the plate. The thickness and the length of the orthotropic square plate are h and a respectively. The principle material axes of the plate in the direction of longitudinal, transverse and normal directions are designated as 1, 2 and 3. The differential equations of the plate with a concentrated load $\bar{P}$ at point (x_q, y_r) are as follows:

$$
\begin{aligned}
&\frac{\partial Q_x}{\partial x}+\frac{\partial Q_y}{\partial y}=-\bar{P}\delta(x-x_q)\delta(y-y_r), \quad \frac{\partial M_x}{\partial x}+\frac{\partial M_{xy}}{\partial y}-Q_x=0,\\
&\frac{\partial M_y}{\partial y}+\frac{\partial M_{xy}}{\partial x}-Q_y=0, \quad M_x=D_{11}\frac{\partial \theta_x}{\partial x}+D_{12}\frac{\partial \theta_y}{\partial y}+D_{16}\left(\frac{\partial \theta_x}{\partial y}+\frac{\partial \theta_y}{\partial x}\right),\\
&M_y=D_{12}\frac{\partial \theta_x}{\partial x}+D_{22}\frac{\partial \theta_y}{\partial y}+D_{26}\left(\frac{\partial \theta_x}{\partial y}+\frac{\partial \theta_y}{\partial x}\right),\\
&M_{xy}=D_{16}\frac{\partial \theta_x}{\partial x}+D_{26}\frac{\partial \theta_y}{\partial y}+D_{66}\left(\frac{\partial \theta_x}{\partial y}+\frac{\partial \theta_y}{\partial x}\right),\\
&Q_y=kA_{44}\left(\frac{\partial w}{\partial y}+\theta_y\right)+kA_{45}\left(\frac{\partial w}{\partial x}+\theta_x\right),\\
&Q_x=kA_{45}\left(\frac{\partial w}{\partial y}+\theta_y\right)+kA_{55}\left(\frac{\partial w}{\partial x}+\theta_x\right),
\end{aligned}
\tag{1}
$$

where Q_x and Q_y are the transverse shear forces, M_x and M_y are the bending moments, M_{xy} is the twisting moment, $k=5/6$ is the shear correction factor, $\delta(x-x_q)$ and $\delta(y-y_r)$ are Dirac's delta functions, A_{ij} is the extensional stiffness ($i, j=4, 5$) and D_{ij} is the bending stiffness ($i, j=1, 2, 6$).

A_{ij} and D_{ij} can be obtained by the following expressions:

$$
\begin{aligned}
&A_{ij}=Q_{ij}h, \quad D_{ij}=\tfrac{1}{12}Q_{ij}h^3, \quad Q_{16}=0, \quad Q_{26}=0, \quad Q_{45}=0,\\
&Q_{11}=\frac{E_1}{1-\nu_{12}\nu_{21}}, \quad Q_{22}=\frac{E_2}{1-\nu_{12}\nu_{21}}, \quad Q_{12}=\frac{\nu_{12}E_2}{1-\nu_{12}\nu_{21}},\\
&Q_{44}=G_{23}, \quad Q_{55}=G_{31}, \quad Q_{66}=G_{12},
\end{aligned}
$$

where E_1 is the axial modulus in the 1-direction, E_2 is the axial modulus in the 2-direction, ν_{12} is the Poisson ratio associated with loading in the 1-direction and strain in the

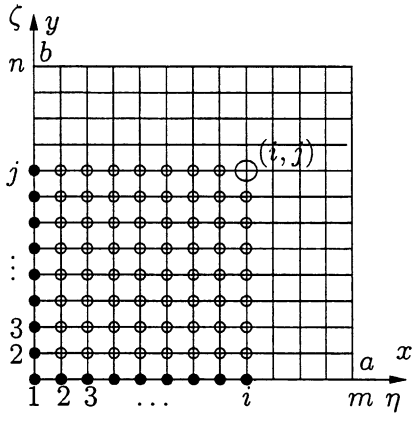

Figure 2. Discrete points on a rectangular plate.

2-direction, v_{21} is the Poisson ratio associated with loading in the 2-direction and strain in the 1-direction, and G_{23}, G_{31} and G_{12} are the shear moduli in 2–3, 3–1 and 1–2 planes.

By using the non-dimensional expressions

$$[X_1, X_2] = \frac{a^2}{D_0(1 - v_{12}v_{21})}[Q_y, Q_x], \quad [X_3, X_4, X_5] = \frac{a}{D_0(1 - v_{12}v_{21})}[M_{xy}, M_y, M_x],$$
$$[X_6, X_7, X_8] = \left[\theta_y, \theta_x, \frac{w}{a}\right], [\eta, \zeta, \xi] = \left[\frac{x}{a}, \frac{y}{b}, \frac{z}{h}\right],$$

where $D_0 = E_2 h_0^3/12(1-v_{12}v_{21})$ is the standard bending rigidity and h_0 is the standard thickness of the plate, equation (1) can be rewritten as

$$\sum_{s=1}^{8}\left\{F_{1ts}\frac{\partial X_s}{\partial \zeta} + F_{2ts}\frac{\partial X_s}{\partial \eta} + F_{3ts}\right\} + P\delta(\eta - \eta_q)\delta(\zeta - \zeta_r)\delta_{1t} = 0, \tag{2}$$

where $t = 1$–8, $P = \bar{P}a/(D_0(1 - v_{12}v_{21}))$, δ_{ij} is Kronecker's delta, and F_{1ts}, F_{2ts} and F_{3ts} are given in Appendix A.

By dividing a rectangular plate vertically into m equal-length parts and horizontally into n equal-length parts as shown in Figure 2, the plate can be considered as a group of discrete points which are the intersections of the $(m+1)$ vertical and $(n+1)$ horizontal dividing lines. In this note, the rectangular area, $0 \leqslant \eta \leqslant \eta_i$, $0 \leqslant \zeta \leqslant \zeta_j$, corresponding to the arbitrary intersection (i, j) as shown in Figure 2 is denoted as the area $[i, j]$, the intersection (i, j) denoted by ○ is called the main point of the area $[i, j]$, the intersections denoted by ○ are called the inner dependent points of the area, and the intersections denoted by ● are called the boundary dependent points of the area.

The discrete solution [14] of the fundamental differential equation (2) is

$$X_{pij} = \sum_{d=1}^{6}\left\{\sum_{f=0}^{i} a_{pijfd}X_{rf0} + \sum_{g=0}^{j} b_{pijgd}X_{s0g}\right\} + \bar{q}_{pij}P, \tag{3}$$

where a_{pijfd}, b_{pijgd} and $\bar{q}_{pij}$ are given in Appendix B, the quantities X_{rf0} ($r = 1, 3, 4, 6, 7, 8$) and X_{s0g} ($s = 2, 3, 5, 6, 7, 8$) are six independent quantities at each boundary dependent point along the horizontal axis and the vertical axis in Figure 2, respectively, and the discrete Green function is chosen as $X_{8ij}/[\bar{P}a/D_0(1 - v_{12}v_{21}]$.

4. CHARACTERISTIC EQUATION OF FREE VIBRATION OF RECTANGULAR PLATE WITH NON-UNIFORM THICKNESS

By applying the Green function $w(x_0, y_0, x, y)/\bar{P}$ which is the displacement at a point (x_0, y_0) of a plate with a concentrated load $\bar{P}$ at a point (x, y) and point support at each discrete point (x_c, y_d), the displacement amplitude $\hat{w}(x_0, y_0)$ at a point (x_0, y_0) of the rectangular plate during the free vibration is given as

$$\hat{w}(x_0, y_0) = \int_0^b \int_0^a \rho h \omega^2 \hat{w}(x, y)[w(x_0, y_0, x, y)/\bar{P}]\, \mathrm{d}x\, \mathrm{d}y, \tag{4}$$

where ρ is the mass density of the plate material.

The following non-dimensional expressions are used:

$$\lambda^4 = \frac{\rho_0 h_0 \omega^2 a^4}{D_0(1 - \nu_{12}\nu_{21})}, \quad H(\eta, \zeta) = \frac{\rho(x, y)}{\rho_0}\frac{h(x, y)}{h_0}, \quad W(\eta, \zeta) = \frac{\hat{w}(x, y)}{a},$$
$$G(\eta_0, \zeta_0, \eta, \zeta) = \frac{w(x_0, y_0, x, y)}{a}\frac{D_0(1 - \nu_{12}\nu_{21})}{\bar{P}a},$$

where ρ_0 is the standard mass density.

By using the numerical integration method, equation (4) is discretely expressed as

$$kW_{kl} = \sum_{i=0}^{m}\sum_{j=0}^{n} \beta_{mi}\beta_{nj}H_{ij}G_{klij}W_{ij} \quad k = 1/(\mu\lambda^4). \tag{5}$$

From equation (5), homogeneous linear equations in $(\mathrm{m}+1)\times(\mathrm{n}+1)$ unknowns W_{00}, $W_{01},\ldots, W_{0n}$, W_{10}, $W_{11},\ldots, W_{1n},\ldots, W_{m0}$, $W_{m1},\ldots, W_{mn}$ are obtained as

$$\sum_{i=0}^{m}\sum_{j=0}^{n}(\beta_{mi}\beta_{nj}H_{ij}G_{klij} - k\delta_{ik}\delta_{jl})W_{ij} = 0 \quad (k = 0, 1, \ldots, m, l = 0, 1, \ldots, n). \tag{6}$$

The characteristic equation of the free vibration of a rectangular plate with variable thickness is obtained from equation (6) as follows:

$$\begin{vmatrix} \mathbf{K}_{00} & \mathbf{K}_{01} & \mathbf{K}_{02} & \ldots & \mathbf{K}_{0m} \\ \mathbf{K}_{10} & \mathbf{K}_{11} & \mathbf{K}_{12} & \ldots & \mathbf{K}_{1m} \\ \mathbf{K}_{20} & \mathbf{K}_{21} & \mathbf{K}_{22} & \ldots & \mathbf{K}_{2m} \\ \vdots & \vdots & \vdots & \ddots & \vdots \\ \mathbf{K}_{m0} & \mathbf{K}_{m1} & \mathbf{K}_{m2} & \ldots & \mathbf{K}_{mm} \end{vmatrix} = 0, \tag{7}$$

where

$$\mathbf{K}_{ij} = \beta_{mj}\begin{vmatrix} \beta_{n0}H_{j0}G_{i0j0} - k\delta_{ij} & \beta_{n1}H_{j1}G_{i0j1} & \ldots & \beta_{nn}H_{jn}G_{i0jn} \\ \beta_{n0}H_{j0}G_{i1j0} & \beta_{n1}H_{j1}G_{i1j1} - k\delta_{ij} & \ldots & \beta_{nn}H_{jn}G_{i1jn} \\ \beta_{n0}H_{j0}G_{i2j0} & \beta_{n1}H_{j1}G_{i2j1} & \ldots & \beta_{nn}H_{jn}G_{i2jn} \\ \vdots & \vdots & \ddots & \vdots \\ \beta_{n0}H_{j0}G_{inj0} & \beta_{n1}H_{j1}G_{inj1} & \ldots & \beta_{nn}H_{jn}G_{injn} - k\delta_{ij} \end{vmatrix}.$$

5. NUMERICAL RESULTS

4.1. CONVERGENCE OF SOLUTION

In order to examine the convergence, numerical calculation is carried out by varying the number of divisions m and n. The lowest eight natural frequency parameters of orthotropic isosceles right triangular plate are shown in Figure 3. The graphite/epoxy material is used. Its properties are given as $E_1/E_2 = 17{\cdot}57$, $G_{12}/E_2 = G_{13}/E_2 = 0{\cdot}7$, $G_{23}/E_2 = 0{\cdot}5$, $v_{12} = 0{\cdot}28$. Figure 4 is used to determine the suitable thickness ratio h/h_t of the original and extremely thin parts. It can be noticed that convergent results can be obtained when m and n are not smaller than 10. It is sufficient to set the thickness ratio $h/h_t \geqslant 5$.

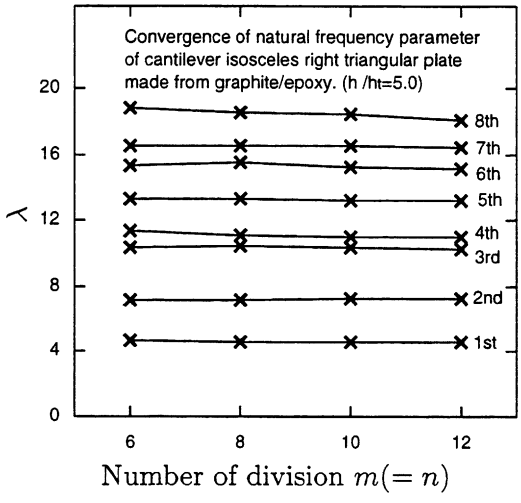

Figure 3. Natural frequency parameter λ versus the number of division m ($=n$) for orthotropic CFF isosceles right triangular plate.

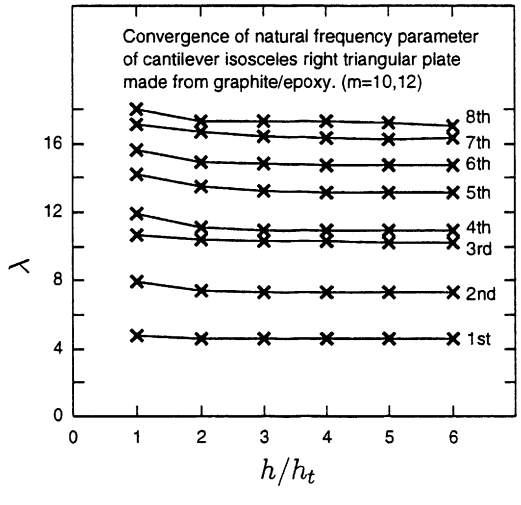

Figure 4. Natural frequency parameter λ versus the thickness ratio h/h_t for orthotropic CFF isosceles right triangular plate.

TABLE 1

Natural frequency parameter λ for CFF isosceles right triangular plate

			Mode sequence number							
b/a	Material	References	1	2	3	4	5	6	7	8
		Present								
		10×10	2·498	4·860	5·850	7·466	9·059	9·980	10·991	11·861
1	Isotropic	12×12	2·507	4·875	5·833	7·502	8·997	9·992	10·910	11·804
		Ex.[†]	2·527	4·908	5·796	7·585	8·856	10·019	10·726	11·672
		Kim [7]	2·542	4·959	5·852	7·672	8·951	10·203	—	—
		Lam [11]	2·540	4·957	5·858	7·873	—	—	—	—
		Present								
		10×10	4·631	7·236	10·355	10·075	13·266	15·283	16·583	18·449
1	Orthotropic	12×12	4·630	7·250	10·331	11·042	13·227	15·123	16·489	18·061
		Ex.	4·628	7·283	10·277	10·967	13·139	14·757	16·275	17·179
		Kim [7]	4·659	7·350	10·398	11·091	13·313	14·968	—	—
		Present								
		10×10	2·432	4·298	5·614	6·283	8·006	8·880	9·564	9·925
1·5	Isotropic	12×12	2·437	4·308	5·589	6·311	7·992	8·811	9·473	9·941
		Ex.	2·447	4·333	5·532	6·374	7·959	8·654	9·266	9·978
		Kim [7]	2·464	4·372	5·588	6·449	8·072	8·828	—	—
		Present								
		10×10	4·486	6·459	8·768	10·765	11·128	13·255	14·198	15·915
1·5	Orthotropic	12×12	4·483	6·457	8·732	10·652	11·036	13·099	14·010	15·548
		Ex.	4·476	6·454	8·652	10·396	10·826	12·719	13·581	14·715
		Kim [7]	4·501	6·506	8·730	10·561	10·896	12·858	—	—

[†] The value obtained by using Richardson's extrapolation formula.

In the present analysis, the thickness ratio $h/h_t = 5$ is used and the convergent values of frequency parameter are obtained by using Richardson's extrapolation formula for two cases of divisional numbers m ($=n$) of 10 and 12.

4.2. ACCURACY OF SOLUTION

4.2.1. *Right triangular plate with uniform thickness*

Numerical solutions for the frequencies of isotropic and orthotropic CFF right isosceles triangular plates with aspect ratios $a/b = 1$ and 1·5 are given in Table 1. For the isotropic plate, $v = 0{\cdot}3$ is used. The present method yields better slightly lower values of frequency parameter as compared with those of Kim and Dickinson [7] and Lam *et al.* [11], which derive from a Rayleigh–Ritz solution. The model lines of eight modes of these plates are shown in Figure 5.

4.2.2. *Right triangular plate with variable thickness*

Table 2 gives the natural frequency parameters for right triangular plate with variable thickness for aspect ratios $b/a = 1$ and 1·5. The thickness varies linearly along the η-axis and is expressed as $h(\eta, \zeta) = h_0(1 - 0{\cdot}5\eta)$. Isotropic and orthotropic cases are considered. The results of isosceles right triangular plate for isotropic case are compared with those obtained by Liew *et al.* [9]. It can be seen that they agree closely.

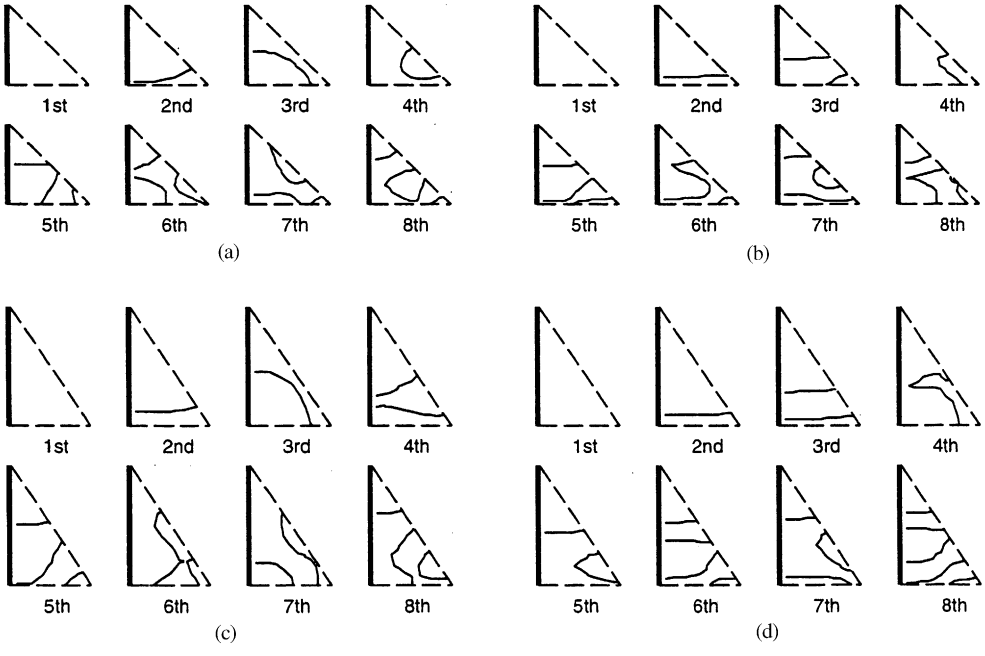

Figure 5. Nodal patterns for CFF isosceles right triangular plate: (a) isotropic plate with $b/a = 1$; (b) orthotropic plate with $b/a = 1$; (c) isotropic plate with $b/a = 1{\cdot}5$; (d) orthotropic plate with $b/a = 1{\cdot}5$.

TABLE 2

Natural frequency parameter λ for CFF isosceles right triangular plate with variable thickness

			Mode sequence number							
B/a	Material	References	1	2	3	4	5	6	7	8
1	Isotropic	Present								
		10×10	2·471	4·520	5·340	6·812	8·098	9·056	9·969	10·895
		12×12	2·486	4·529	5·339	6·816	8·023	9·039	9·868	10·743
		Ex.	2·519	4·549	5·337	6·826	7·854	9·001	9·636	10·398
		Liew [9]	2·582	4·636	5·479	6·906	8·002	9·186	—	—
1	Orthotropic	Present								
		10×10	4·575	6·873	9·520	10·008	12·164	13·992	15·259	16·007
		12×12	4·588	6·891	9·472	9·994	12·091	13·805	15·023	15·696
		Ex.	4·616	6·931	9·361	9·963	11·922	13·380	14·485	14·988
1·5	Isotropic	Present								
		10×10	2·401	4·039	5·050	5·809	7·292	7·990	8·524	9·060
		12×12	2·411	4·050	5·033	5·816	7·251	7·912	8·439	9·036
		Ex.	2·436	4·076	4·996	5·832	7·157	7·735	8·247	8·982
1·5	Orthotropic	Present								
		10×10	4·442	6·145	8·211	9·585	10·384	12·113	13·108	14·960
		12×12	4·450	6·153	8·157	9·517	10·223	11·918	12·809	14·357
		Ex.	4·470	6·173	8·036	9·361	9·859	11·476	12·128	12·987

5. CONCLUSIONS

An approximate method has been proposed for the free vibration of orthotropic right cantilever triangular plate with various aspect ratios and variable thickness. An equivalent rectangular is used to replace the right triangular plate in the free vibration analysis. Based on the Green function of the equivalent rectangular plate, the characteristic equation of free vibration is obtained. The lower eight values of frequency parameter and their mode shapes are given. These results show that the numerical solutions obtained by the proposed method have a good convergence and satisfactory accuracy.

ACKNOWLEDGMENTS

The present study was sponsored by the Japan Society for the Promotion of Science (JSPS).

REFERENCES

1. A. H. Leissa 1969 *Vibration of Plates* (NASA SP-160). Washington, DC: Office of Technology Utilization, NASA.
2. D. J. Gorman 1983 *Journal of Sound and Vibration* **89**, 107–118. A highly accurate analytical solution for free vibration analysis of simply supported right triangular plates.
3. D. J. Gorman 1986 *Journal of Sound and Vibration* **106**, 419–431. Free vibration analysis of right triangular plates with combinations of clamped–simply supported boundary conditions.
4. D. J. Gorman 1987 *Journal of Sound and Vibration* **112**, 173–176. A modified superposition method for the free vibration analysis of right triangular plates.
5. H. T. Saliba 1990 *Journal of Sound and Vibration* **139**, 289–297. Transverse free vibration of simply supported right triangular thin plates: a highly accurate simplified solution.
6. H. T. Saliba 1995 *Journal of Sound and Vibration* **183**, 765–778. Transverse free vibration of right triangular thin plates with combinations of clamped and simply supported boundary conditions: a highly accurate simplified solution.
7. C. S. Kim and S. M. Dickinson 1990 *Journal of Sound and Vibration* **141**, 291–311. The free flexural vibration of right triangular isotropic and isotropic plates.
8. S. Mirza and M. Bijlani 1985 *Computers and Structures* **21**, 1129–1135. Vibration of triangular plates of variable thickness.
9. K. M. Liew, C. W. Lim and M. K. Lim 1994 *Journal of Sound and Vibration* **177**, 479–501. Transverse vibration of trapezoidal plates of variable thickness: unsymmetric trapezoids.
10. O. G. Mcgee and G. T. Giaimo 1992 *Journal of Sound and Vibration* **159**, 279–293. Three-dimensional vibrations of cantilevered right triangular plates.
11. K. Y. Lam, K. M. Liew and S. T. Chow 1990 *International Journal of Mechanical Science* **32**, 455–464. Free vibrations analysis of isotropic and orthotropic triangular plates.
12. S. K. Malhotra, N. Ganesan and M. A. Veluswami 1989 *Composite Structures* **12**, 17–25. Vibrations of orthotropic triangular plates.
13. D. V. Bambill, P. A. A. Laura and R. E. Rossi 1998 *Journal of Sound and Vibration* **210**, 286–290. Transverse vibrations of rectangular, trapezoidal and triangular orthotropic, cantilever plates.
14. T. Sakiyama and M. Huang 1998 *Journal of Sound and Vibration* **216**, 379–397. Free vibration analysis of rectangular plates with variable thickness.
15. I. M. Daniel and O. Ishai 1994 *Engineering Mechanics of Composite Materials*. Oxford: Oxford University Press.

APPENDIX A

$$F_{111} = F_{123} = F_{134} = 1, \quad F_{146} = \bar{D}_{12}, \quad F_{147} = \bar{D}_{16},$$
$$F_{156} = \bar{D}_{22}, \quad F_{157} = F_{166} = \bar{D}_{26}, \quad F_{167} = \bar{D}_{66}, \quad F_{178} = k\bar{A}_{44}, \quad F_{188} = k\bar{A}_{45},$$

$$F_{212} = F_{225} = F_{233} = \mu, \quad F_{246} = F_{267} = \mu\bar{D}_{16}, F_{247} = \mu\bar{D}_{11},$$

$$F_{256} = \mu\bar{D}_{26}, \quad F_{257} = \mu\bar{D}_{12}, \quad F_{266} = \mu\bar{D}_{66},$$

$$F_{278} = F_{30907} = F_{31006} = \mu k\bar{A}_{45}, \quad F_{288} = F_{387} = \mu k\bar{A}_{55},$$

$$F_{322} = F_{331} = -\mu, \quad F_{345} = F_{354} = F_{363} = -\mu\bar{D}F_{371} = F_{382} = -\mu\overline{DT},$$

other $F_{kts} = 0$.

APPENDIX B

$$A_{p1} = \gamma_{p1}, \quad A_{p2} = 0, \quad A_{p3} = \gamma_{p2}, \quad A_{p4} = \gamma_{p3}, \quad A_{p5} = 0,$$

$$A_{p6} = \bar{D}_{12}\gamma_{p4} + \bar{D}_{22}\gamma_{p5} + \bar{D}_{26}\gamma_{p6}, \quad A_{p7} = \bar{D}_{16}\gamma_{p06} + \bar{D}_{26}\gamma_{p07} + \bar{D}_{66}\gamma_{p08},$$

$$A_{p8} = k(\bar{A}_{44}\gamma_{p7} + \bar{A}_{45}\gamma_{p8}), \quad B_{p1} = 0, \quad B_{p2} = \mu\gamma_{p1}, \quad B_{p3} = \mu\gamma_{p3}, \quad B_{p4} = 0, \quad B_{p5} = \mu\gamma_{p2},$$

$$B_{p6} = \mu(\bar{D}_{16}\gamma_{p4} + \bar{D}_{26}\gamma_{p5} + \bar{D}_{66}\gamma_{p6}), \quad B_{p7} = \mu(\bar{D}_{11}\gamma_{p4} + \bar{D}_{12}\gamma_{p5} + \bar{D}_{16}\gamma_{p6}),$$

$$B_{p8} = \mu k(\bar{A}_{45}\gamma_{p7} + \bar{A}_{55}\gamma_{p8}), C_{p1kl} = \mu\gamma_{p3} + \mu\overline{DT}_{kl}\gamma_{p7}, C_{p2kl} = \mu\gamma_{p2} + \mu\overline{DT}_{kl}\gamma_{p8},$$

$$C_{p3kl} = \mu\bar{D}_{kl}\gamma_{p6}, C_{p4kl} = \mu\bar{D}_{kl}\gamma_{p7}, \quad C_{p5kl} = \mu\bar{D}_{kl}\gamma_{p4}, \quad C_{p6kl} = -\mu k(\bar{A}_{44}\gamma_{p7} + \bar{A}_{45}\gamma_{p8}),$$

$$C_{p7kl} = -\mu k(\bar{A}_{45}\gamma_{p7} + \bar{A}_{55}\gamma_{p8}), C_{p8kl} = 0, \quad [\gamma_{pt}] = [\rho_{tp}]^{-1},$$

$$\rho_{11} = \beta_{ii}, \ \rho_{12} = -\mu\beta_{jj}, \quad \rho_{22} = -\mu\beta_{ij}, \rho_{23} = \beta_{ii}, \quad \rho_{25} = \mu\beta_{jj}, \quad \rho_{31} = -\mu\beta_{ij}, \quad \rho_{33} = \mu\beta_{jj},$$

$$\rho_{34} = \beta_{ii}, \quad \rho_{45} = -\mu\beta_{ij}\bar{D}_{ij}, \ \rho_{46} = \bar{D}_{12}\beta_{ii} + \mu\bar{D}_{16}\beta_{jj}, \quad \rho_{47} = \bar{D}_{16}\beta_{ii} + \mu\bar{D}_{11}\beta_{jj},$$
$$\rho_{54} = -\mu\beta_{ij}\bar{D}_{ij}, \ \rho_{56} = \bar{D}_{22}\beta_{ii} + \mu\bar{D}_{26}\beta_{jj}, \quad \rho_{57} = \bar{D}_{26}\beta_{ii} + \mu\bar{D}_{12}\beta_{jj},$$

$$\rho_{63} = -\mu\beta_{ij}\bar{D}_{ij}, \quad \rho_{666} = \bar{D}_{26}\beta_{ii} + \mu\bar{D}_{66}\beta_{jj}, \ \rho_{67} = \bar{D}_{66}\beta_{ii} + \mu\bar{D}_{16}\beta_{jj}, \quad \rho_{71} = -\mu\beta_{ij}\bar{D}_{ij},$$

$$\rho_{76} = \mu k\bar{A}_{44}\beta_{ij}, \quad \rho_{77} = \mu k\bar{A}_{45}\beta_{ij}, \quad \rho_{78} = k(\bar{A}_{44}\beta_{ii} + \mu\bar{A}_{45}\beta_{jj}), \quad \rho_{82} = -\mu\beta_{ij}\bar{D}_{ij},$$
$$\rho_{86} = \mu k\bar{A}_{45}\beta_{ij}, \quad \rho_{87} = \mu k\bar{A}_{55}\beta_{ij}, \quad \rho_{88} = k(\bar{A}_{45}\beta_{ii} + \mu\bar{A}_{55}\beta_{ij}), \quad \text{other} \quad \rho_{tp} = 0,$$
$$a_{1i0i01} = a_{3i0i02} = a_{4i0i03} = a_{6i0i04} = a_{7i0i05} = a_{8i0i06},$$

$$b_{20jj01} = b_{30jj02} = b_{50jj03} = -b_{60jj04} = b_{70jj05} = b_{80jj06}, \quad b_{300002} = 0,$$

$$a_{pijfd} = \sum_{t=1}^{13}\left\{\sum_{k=0}^{i}\beta_{ik}A_{pt}[a_{tk0fd} - a_{tkjfd}(1-\delta_{ki})] + \sum_{l=0}^{j}\beta_{jl}B_{pt}[a_{t0lfd} - a_{tilfd}(1-\delta_{lj})]\right.$$
$$\left. + \sum_{k=0}^{i}\sum_{l=0}^{j}\beta_{ik}\beta_{jl}C_{ptkl}a_{tklfd}(1-\delta_{ki}\delta_{lj})\right\},$$

$$b_{pijfd} = \sum_{t=1}^{13}\Bigg\{\sum_{k=0}^{i}\beta_{ik}A_{pt}[b_{tk0gd} - b_{tkjgd}(1-\delta_{ki})] + \sum_{l=0}^{j}\beta_{jl}B_{pt}[b_{t0lgd} - b_{tilgd}(1-\delta_{lj})] + \sum_{k=0}^{i}\sum_{l=0}^{j}\beta_{ik}\beta_{jl}C_{ptkl}b_{tklgd}(1-\delta_{ki}\delta_{lj})\Bigg\},$$

$$\bar{q}_{pij} = \sum_{t=1}^{13}\Bigg\{\sum_{k=0}^{i}\beta_{ik}A_{pt}[\bar{q}_{tk0} - \bar{q}_{tkj}(1-\delta_{ki})] + \sum_{l=0}^{i}\beta_{jl}B_{pt}[\bar{q}_{t0l} - \bar{q}_{til}(1-\delta_{lj})] + \sum_{k=0}^{i}\sum_{l=0}^{j}\beta_{ik}\beta_{jl}C_{ptkl}\bar{q}_{tkl}(1-\delta_{ki}\delta_{lj})\Bigg\} - A_{p1}u_{iq}u_{jr}.$$